Supplemental Information

Coupling Effects of Thermodynamics in Multiple Ion Co-Precipitation for Precursor towards Layered Oxide Cathode

He Zhao[a], Qi Zhang[b], Xuan-Wen Gao[a]*, Jian-Zhong Li[a], Hua-Kun Liu[b], Wen-Bin Luo[a,b,]*

[a]School of Metallurgy, Northeastern University, Shenyang, 110819, China

[b]Institute for Superconducting and Electronic Materials, University of Wollongong, Squires Way, Fairy Meadow, NSW 2500, Australia

Table S1. Ion concentration of liquid supernatant on manganese carbonate.

Ion	Mn^{2+}	Na^{+}	CO_3^{2-}	SO_4^{2-}	OH^{-}
Concentration (mol•L-1)	1.11×10^{-5}	0.56	0.014	0.2664	5.37×10^{-5}

Table S2. Ion concentration of liquid supernatant on cobalt carbonate.

Ion	Co^{2+}	Na^{+}	CO_3^{2-}	SO_4^{2-}	OH^{-}
Concentration (mol•L-1)	9.11×10^{-6}	0.136	0.132	0.2664	4.27×10^{-5}

Table S3. Ion concentration of liquid supernatant on nickel carbonate.

Ion	Ni^{2+}	Na^{+}	CO_3^{2-}	SO_4^{2-}	OH^{-}
Concentration (mol•L-1)	1.24×10^{-5}	0.136	0.132	0.2664	4.56×10^{-5}

Table S4. Table of different ion concentrations in liquid supernatant.

Ion	Mn^{2+}	Ni^{2+}	Co^{2+}	Na^{+}	OH^{-}	CO_3^{2-}	SO_4^{2-}
Concentration (mol•L-1)	3.96×10^{-6}	7.16×10^{-6}	2.55×10^{-6}	0.412	1.18×10^{-5}	6.30×10^{-6}	0.20

Table S5. Ion concentrations of liquid supernatant.

Ion / Al	Na^{+}	Mn^{2+}	Co^{2+}	Ni^{2+}	Al^{3+}	SO_4^{2-}	OH^{-}	CO_3^{2-}
0	0.412	3.961×10^{-6}	2.55×10^{-6}	7.16×10^{-6}	0	0.2	1.18×10^{-5}	0.0063
0.0025	0.4378	1.03×10^{-6}	6.79×10^{-6}	5.28×10^{-6}	3.33×10^{-6}	0.2	8.51×10^{-7}	0.0189
0.005	0.4256	1.24×10^{-6}	1.51×10^{-5}	3.92×10^{-6}	5.19×10^{-6}	0.2011	1.07×10^{-6}	0.0117
0.0075	0.4620	9.1×10^{-7}	2.65×10^{-6}	1.70×10^{-6}	4.08×10^{-6}	0.1996	7.40×10^{-7}	0.031

Table S6. The degree of supersaturation of ions (S) in the solution.

Ion / Supersaturation	Mn^{2+}	Ni^{2+}	Co^{2+}	Al^{3+}
S0	1.40×10^4	69	1.16×10^6	0
Sa	1081.5	15.12	9.17×105	6.85×10^9
Sb	806	6.95	1.26×10^6	2.12×10^{10}
Sc	1567.2	7.98	5.87×10^6	5.5×10^9

Table S7. The Gibbs free energy (ΔG) change in the co-precipitation.

Product / ΔG（J/mol）	$MnCO_3$	$NiCO_3$	$CoCO_3$	$Al(OH)_3$
ΔG0	− 23664	− 10495	− 34614	0
ΔGa	-17317.3	-6732.5	-34030.4	-56135.5
ΔGb	-16588.5	-4805.8	-34819.0	-58939.5
ΔGc	-18236.8	-5148.4	-38633.3	-55595.0

Table S8. XRD refinement data.

Al Content	a (Å)	b (Å)	c (Å)
0	4.929196	8.553962	5.020555
0.0025	4.928775	8.554627	5.021639
0.005	4.928503	8.554564	5.021123
0.0075	4.928179	8.554638	5.020807

Table S9. Summary of EIS results.

Samples	RW (Ω)	R1 (Ω)	R2 (Ω)
x=0	2.589E-002	5.148E+000	1.131E+002
x= 0.0025	5.116E-003	3.928E+000	2.051E+002
x=0.005	2.951E-002	4.673E+000	7.351E+001
x= 0.0075	7.342E-003	5.555E+000	1.351E+002

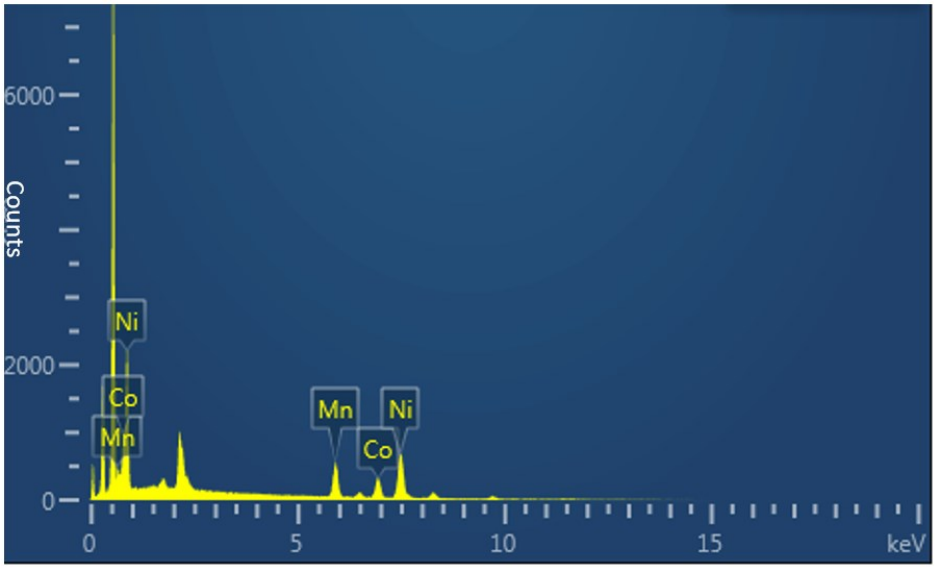

Figure S1. The SEM-EDS spectra of the precursor without Al^{3+} ion.

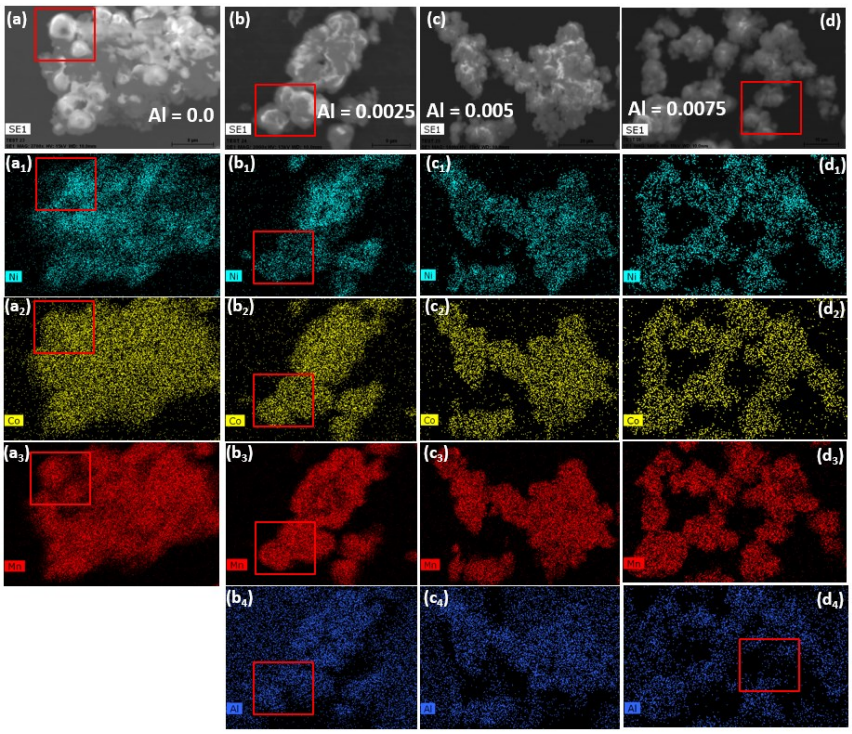

Figure S2. Various element distributions in the precursor as the added Al^{3+} ion content changes from 0 (a) to 0.0025 (b), 0.005 (c), and 0.0075 (d).

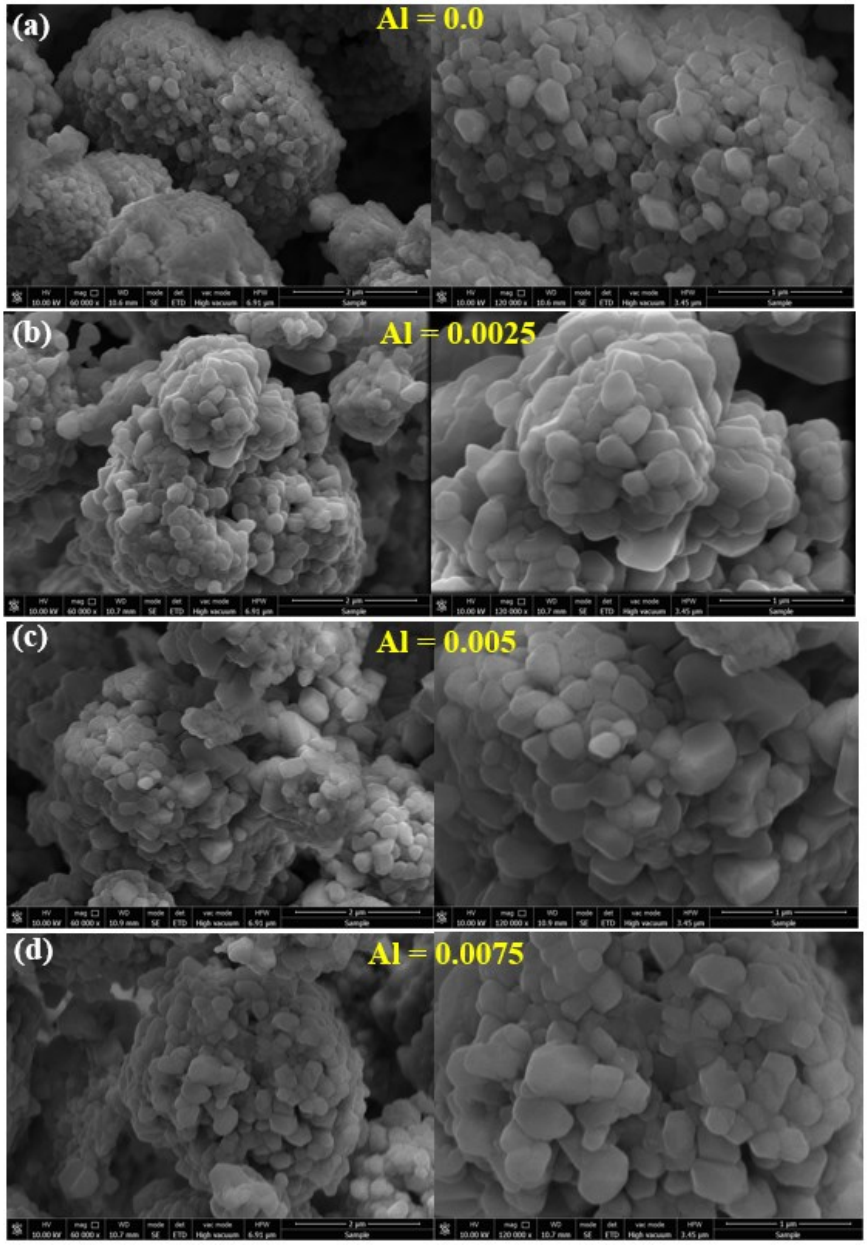

Figure S3. FESEM images of Li[Li0.2Mn0.54Ni0.13Co0.13-xAlx]O2 with different amounts of Al element: 0 (a) to 0.0025 (b), 0.005 (c) and 0.0075 (d).

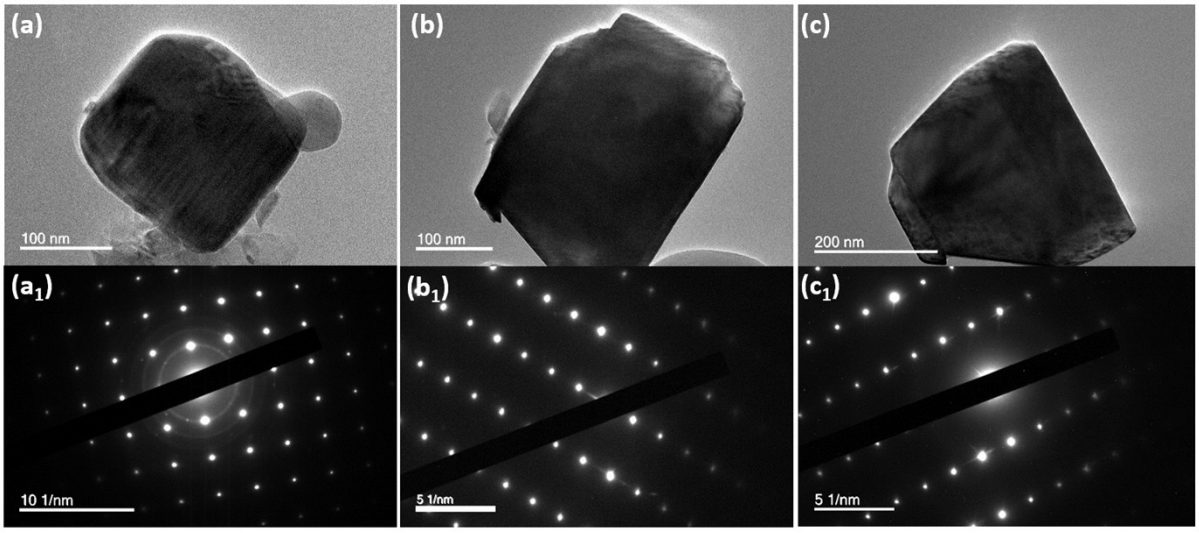

Figure S4. TEM images and SAED patterns of Li[Li0.2Mn0.54Ni0.13Co0.13-xAlx]O2 with different amounts of Al element: 0 (a) to 0.005 (b) and 0.0075 (c).

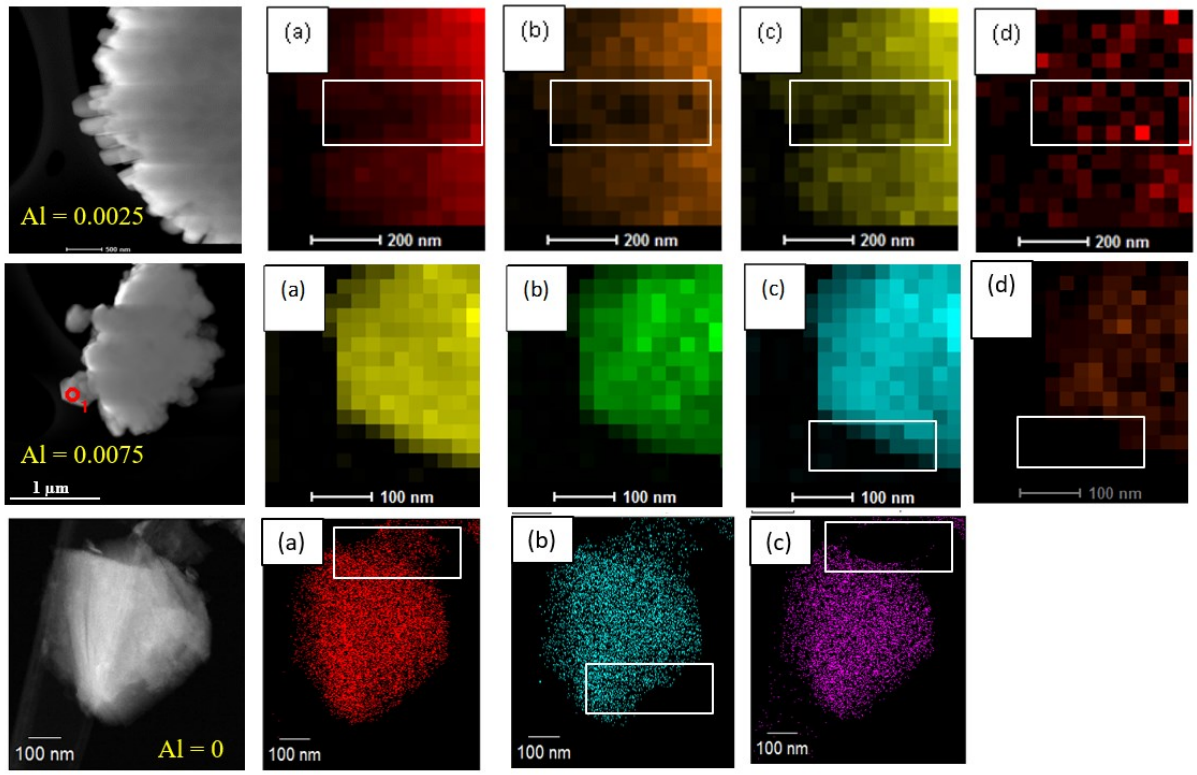

Figure S5. TEM-EDS images of Li[Li0.2Mn0.54Ni0.13Co0.13-xAlx]O2 with different amounts of Al element: 0 to 0.005 and 0.0075; (a) Co; (b) Ni; (c) Mn; (d) Al.

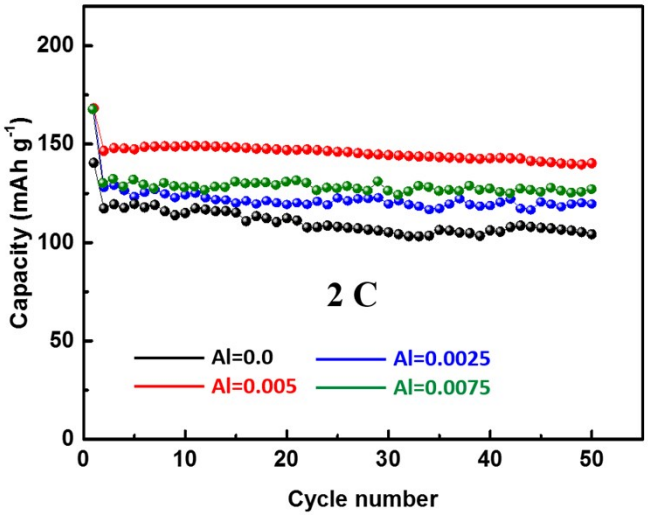

Figure S6. Cycling performance of $Li[Li_{0.2}Mn_{0.54}Ni_{0.13}Co_{0.13-x}Al_x]O_2$ at 2C.